Probing the P-wave charmonium decays of B_c meson

Zhou Rui*

College of Sciences, North China University of Science and Technology, Tangshan 063009, China

(Received 31 December 2017; published 12 February 2018)

Motivated by the large number of B_c meson decay modes observed recently by several detectors at the LHC, we present a detailed analysis of the B_c meson decaying to the P-wave charmonium states and a light pseudoscalar (P) or vector (V) meson within the framework of perturbative QCD factorization. The P-wave charmonium distribution amplitudes are extracted from the $n = 2$, $l = 1$ Schrödinger states for a Coulomb potential, which can be taken as the universal nonperturbative objects to analyze the hard exclusive processes with P-wave charmonium production. It is found that these decays have large branching ratios of the order of $10^{-5} \sim 10^{-2}$, which seem to be in the reach of future experiments. We also provide predictions for the polarization fractions and relative phases of $B_c \to (\chi_{c1}, \chi_{c2}, h_c)V$ decays. It is expected that the longitudinal polarization amplitudes dominate the branching ratios according to the quark helicity analysis, and the magnitudes and phases of parallel polarization amplitude are approximately equal to the perpendicular ones. The obtained results are compared with available experimental data, our previous studies, and numbers from other approaches.

DOI: 10.1103/PhysRevD.97.033001

I. INTRODUCTION

In the quark model, P-wave charmonium states are expected as the orbital excitation of the $c\bar{c}$ assignments with the orbital angular momentum $L = 1$. Since the charm-anticharm quarks pair can be in the spin singlet or spin triplet states, in terms of the spectroscopic notation $^{2s+1}L_J$, there are four types of P-wave charmonium states, namely, $\chi_{c0}(^3P_0)$, $\chi_{c1}(^3P_1)$, $\chi_{c2}(^3P_2)$, and $h_c(^1P_1)$. The current experimental knowledge of these P-wave charmonium states is summarized in Table I [1]. Experimentally the productions of these P-wave charmonium states have been seen in the hadronic B decays: $B \to \chi_{c1}\pi$ [2,3], $B \to \chi_{c0}K^*$ [4,5], $B \to \chi_{c1,c2}K^{(*)}$ [6–10], $B \to h_cK^{(*)}$ [11,12], $B_s \to \chi_{c1}\phi$ [13], $B \to \chi_{c1,c2}K\pi$ [14,15], $B \to \chi_{c1,c2}\pi\pi K$ [15], and in Λ_b^0 baryon decay: $\Lambda_b^0 \to \chi_{c1,c2}pK^-$ [16]. As for hadronic B_c decays, the first evidence of $B_c^+ \to \chi_{c0}(\to K^+K^-)\pi^+$ [17] is reported with a significance of 4.0 standard deviations by the LHCb experiment. The measured product of the ratio of cross sections and branching fraction is

$$\frac{\sigma_{B_c^+}}{\sigma_{B^+}} \times \mathcal{B}(B_c^+ \to \chi_{c0}\pi^+) = (9.8^{+3.4}_{-3.0}(\text{stat}) \pm 0.8(\text{syst})) \times 10^{-6}, \tag{1}$$

where $\sigma_{B_c^+}(\sigma_{B^+})$ is the production cross sections for $B_c(B)$ meson.

As is well known, the pseudoscalar B_c is composed of two heavy-flavored quarks and thus represents a unique laboratory to study heavy-quark dynamics and CP violation. Since each of the two heavy quarks can decay with the other as a spectator, the B_c meson has rich decay channels, and offers a promising opportunity to study nonleptonic weak decays of heavy mesons, to test the standard model (SM), and even to reveal any new physics beyond SM. Decays of B_c mesons to the final states including a charmonium meson are of special interest. First, these decay modes provide a sensitive laboratory for studying strong interaction effects in a heavy meson system. Second, those decays involve two energy scales, the bottom quark mass m_b and charm quark mass m_c. The higher order corrections within the framework of quantum chromodynamics (QCD), described by the expansion of m_c/m_b rather than Λ_{QCD}/m_b with Λ_{QCD} is the QCD scale, may be relatively large, and therefore are more subtle in theoretical studies. Third, one can search for charmonium and charmoniumlike exotic states in one of the intermediate final

TABLE I. The properties of P-wave charmonium states [1].

Mesons	$n^{2s+1}L_J$	J^{PC}	Mass (MeV)	Width (MeV)
χ_{c0}	1^3P_0	0^{++}	3414.75 ± 0.31	10.5 ± 0.6
χ_{c1}	1^3P_1	1^{++}	3510.66 ± 0.07	0.84 ± 0.04
χ_{c2}	1^3P_2	2^{++}	3556.20 ± 0.11	1.93 ± 0.11
h_c	1^1P_1	1^{+-}	3525.38 ± 0.11	0.7 ± 0.4

*jindui1127@126.com

states such as $\chi_{cJ}\pi$ and $\chi_{cJ}\pi\pi$ ($J = 0, 1, 2$), which may be important to understand the detailed dynamics of the multibody B_c decay modes. Besides, such B_c decays provide a direct probe of charmonium properties by reconstructing the charmonium state from its decay to some known final state.

Phenomenologically the B_c meson decays into various charmonium states have been widely studied in the literature. Earlier, a lot of work has been done in the semileptonic and nonleptonic [18–29] decays of the meson B_c to S-wave charmonium mesons. Also, the P-wave charmonium decays of B_c meson have been considered previously by other authors [30–39]. Furthermore, some semileptonic and nonleptonic decays of B_c into the D-wave charmonium states have been analyzed in the framework of the instantaneous Bethe-Salpeter method [40]. More recently, the exclusive decays of the B_c meson into P-wave orbitally excited charmonium and a light meson have been investigated using the nonrelativistic QCD effective theory [41], where the next-to-leading order relativistic corrections to the corresponding form factors are considered.

As a successive work of [42,43], in the present work we will focus on the B_c decays involving a P-wave charmonium state and a light pseudoscalar or vector meson in the final states employing the Perturbative QCD (PQCD) approach based on the k_T factorization theorem. Similar to the case of S-wave charmonium states [44], the P-wave charmonium distribution amplitudes (DAs) can also be expressed as an associated factor, extracted from the P-wave Schrödinger states for a Coulomb potential, multiply by the asymptotic models of the corresponding twists for light mesons. With the help of P-wave DAs, we can make quantitative predictions here, and provide a ready reference to existing and forthcoming experiments.

The rest of this article is organised in the following way. In Sec. II, the Hamiltonian and kinematics, and the P-wave charmonium DAs are shown in cases of scalar, axial-vector, and tensor states. Then the calculations of these decay amplitudes in the PQCD framework are briefly reviewed. In Sec. III, the adopted parameters, numerical results and discussion are given in detail. Finally, the conclusions are given in Sec. IV. The evaluation of the P-wave charmonium distribution amplitudes is relegated to the Appendix.

II. FORMALISM

A. Hamiltonian and kinematics

The effective Hamiltonian describing the B_c nonleptonic decays into charmonium and a light pseudoscalar or vector meson is given by [45]

$$\mathcal{H}_{\rm eff} = \frac{G_F}{\sqrt{2}} V_{cb}^* V_{uq} [C_1(\mu) O_1(\mu) + C_2(\mu) O_2(\mu)], \quad (2)$$

where $q = s, d$ stands for a down type light quark. G_F is the Fermi constant. V_{cb}^* and V_{uq} are the Cabibbo-Kobayashi-Maskawa (CKM) matrix elements. $C_{1,2}(\mu)$ are the perturbatively calculable Wilson coefficients, which encode the short-distance effects above the renormalization scale μ, while $O_{1,2}(\mu)$ are the corresponding local four-quark operators, whose expressions read as

$$\begin{aligned} O_1(\mu) &= \bar{b}_\alpha \gamma^\nu (1-\gamma_5) c_\beta \otimes \bar{u}_\beta \gamma_\nu (1-\gamma_5) q_\alpha, \\ O_2(\mu) &= \bar{b}_\alpha \gamma^\nu (1-\gamma_5) c_\alpha \otimes \bar{u}_\beta \gamma_\nu (1-\gamma_5) q_\beta, \end{aligned} \quad (3)$$

where α and β are color indices and the summation convention over repeated indices is understood. Since the Hamiltonian involves four different flavor quarks, it means that these decays are uncontaminated by the contributions from the penguin operators, and thus the direct CP asymmetries are absent naturally.

The calculation is carried out in the rest frame of B_c meson, the B_c meson momentum P_1, the recoiled charmonium meson momentum P_2, and the ejected light meson momentum P_3 are defined in the light cone coordinates as

$$\begin{aligned} P_1 &= \frac{M}{\sqrt{2}}(1, 1, \mathbf{0}_{\rm T}), \qquad P_2 = \frac{M}{\sqrt{2}}(1 - r_3^2, r_2^2, \mathbf{0}_{\rm T}), \\ P_3 &= \frac{M}{\sqrt{2}}(r_3^2, 1 - r_2^2, \mathbf{0}_{\rm T}), \end{aligned} \quad (4)$$

with the mass ratio $r_{2,3} = m_{2,3}/M$ and M (m_2) is the B_c (charmonium) meson mass, while m_3 is the (chiral) mass of the (pseudoscalar) vector meson. The momentum of the valence quarks $k_{1,2,3}$, whose notation is displayed in Fig. 1, is parametrized as

$$k_1 = x_1 P_1 + \mathbf{k}_{1\rm T}, \qquad k_2 = x_2 P_2 + \mathbf{k}_{2\rm T}, \qquad k_3 = x_3 P_3 + \mathbf{k}_{3\rm T}, \quad (5)$$

where k_{iT}, x_i represent the transverse momentum and longitudinal momentum fraction of the quark/anti-quark inside the meson. When the final states contain a axial-vector charmonium and a vector meson, the longitudinal polarization vectors ϵ_L and transverse polarization vectors ϵ_T can be defined as

$$\begin{aligned} \epsilon_{2L} &= \frac{1}{\sqrt{2(1-r_3^2)} r_2}(1 - r_3^2, -r_2^2, \mathbf{0}_{\rm T}), \qquad \epsilon_{2T} = (0, 0, \mathbf{1}_{\rm T}), \\ \epsilon_{3L} &= \frac{1}{\sqrt{2(1-r_2^2)} r_3}(-r_3^2, 1 - r_2^2, \mathbf{0}_{\rm T}), \qquad \epsilon_{3T} = (0, 0, \mathbf{1}_{\rm T}), \end{aligned} \quad (6)$$

which satisfy the normalization $\epsilon_L^2 = \epsilon_T^2 = -1$ and the orthogonality $\epsilon_{2L} \cdot P_2 = \epsilon_{3L} \cdot P_3 = 0$.

For a tensor charmonium, the polarization tensor $\epsilon_{\mu\nu}(\lambda)$ with helicity λ can be constructed via the polarization vector ϵ_μ [46,47]:

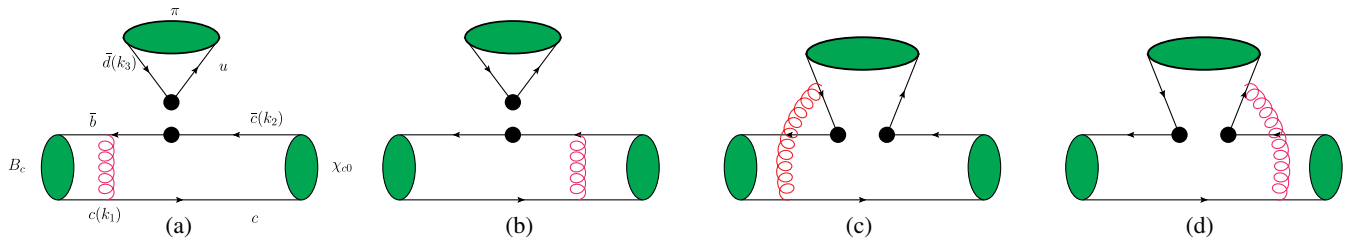

FIG. 1. The typical leading-order Feynman diagrams for the decay $B_c \to \chi_{c0}\pi$. (a,b) The factorizable diagrams, and (c,d) the nonfactorizable diagrams.

$$\begin{aligned}
\epsilon_{\mu\nu}(\pm 2) &= \epsilon_\mu(\pm)\epsilon_\nu(\pm),\\
\epsilon_{\mu\nu}(\pm 1) &= \frac{1}{\sqrt{2}}[\epsilon_\mu(\pm)\epsilon_\nu(0) + \epsilon_\nu(\pm)\epsilon_\mu(0)],\\
\epsilon_{\mu\nu}(0) &= \frac{1}{\sqrt{6}}[\epsilon_\mu(+)\epsilon_\nu(-) + \epsilon_\mu(-)\epsilon_\nu(+)]\\
&\quad + \sqrt{\frac{2}{3}}\epsilon_\mu(0)\epsilon_\nu(0),
\end{aligned} \tag{7}$$

with $\epsilon(\pm) = \epsilon_{2T}$ and $\epsilon(0) = \epsilon_{2L}$. It is convenient to define another polarization vector $\epsilon_{\bullet\mu}(\lambda) = m_2 \frac{\epsilon_{\mu\nu(\lambda)} v^\nu}{P_2\cdot v}$, which satisfy

$$\begin{aligned}
&\epsilon_{\bullet\mu}(\pm 2) = 0, \qquad \epsilon_{\bullet\mu}(\pm 1) = m_2\sqrt{\frac{1}{2}}\frac{\epsilon_{2L}\cdot v}{P_2\cdot v}\epsilon_{2T\mu},\\
&\epsilon_{\bullet\mu}(0) = m_2\sqrt{\frac{2}{3}}\frac{\epsilon_{2L}\cdot v}{P_2\cdot v}\epsilon_{2L\mu}.
\end{aligned} \tag{8}$$

The contraction is evaluated as $\frac{\epsilon_{2L}\cdot v}{P_2\cdot v} = \frac{1}{m_2}$ by neglecting the light meson mass, then we get the relations $\epsilon_{\bullet T} = \epsilon_\bullet(\pm 1) = \sqrt{\frac{1}{2}}\epsilon_{2T}$ and $\epsilon_{\bullet L} = \epsilon_\bullet(0) = \sqrt{\frac{2}{3}}\epsilon_{2L}$. Note that $\epsilon_\bullet$ has the same energy scaling as the usual polarization vector of a vector meson. It makes the calculations of B_c decays into a tensor meson are similar to those of vector analogues by replacing the polarization vector with the corresponding $\epsilon_\bullet$.

B. Mesons wave function and the distribution amplitudes

In the considered decays, there are three typical scales: M, m_2, and the heavy-meson and heavy-quark mass difference $\bar{\Lambda}$. They allow for a consistent power expansion in m_2/M and in $\bar{\Lambda}/m_2$ under the hierarchy of $\bar{\Lambda} \ll m_2 \ll M$. In the heavy-quark and large-recoil limits, based on the k_T factorization theorem, the decay amplitudes are expressed as the convolution of the hard kernels with the relevant meson wave functions. The hard kernels can be treated by perturbative QCD at the leading order in an α_s expansion (single gluon exchange as depicted in Fig. 1). The higher-order radiative corrections generate the logarithm divergences, which can be absorbed into the meson wave functions. One also encounters double logarithm divergences when collinear and soft divergences overlap, which can be summed to all orders to give a Sudakov factor. After absorbing all the soft dynamics, the initial and final state meson wave functions can be treated as nonperturbative inputs, which are not calculable but universal.

Analogous to the B meson [48], up to first order in $1/M$ under above hierarchy, the B_c meson wave functions are decomposed into the following Lorentz structures [49,50]:

$$\begin{aligned}
&\int d^4z e^{ik_1\cdot z}\langle 0|\bar{b}_\alpha(0)c_\beta(z)|B_c(P_1)\rangle\\
&= \frac{i}{\sqrt{2N_c}}\left\{(P_1\!\!\!/ + M)\gamma_5\left[\phi_{B_c}(k_1) - \frac{n\!\!\!/ - v\!\!\!/}{\sqrt{2}}\bar{\phi}_{B_c}(k_1)\right]\right\}_{\beta\alpha}
\end{aligned} \tag{9}$$

with the two lightlike vectors $n = (1, 0, \mathbf{0}_T)$ and $v = (0, 1, \mathbf{0}_T)$. $N_c = 3$ is the color factor. Here, we only consider the dominant Lorentz structure from the first term, while the second Lorentz structure starting from the next-to-leading-power $\bar{\Lambda}/M$ is numerically neglected [51,52]. In coordinate space the distribution amplitude ϕ_{B_c} is adopted in the form [53]

$$\phi_{B_c}(x) = N_B x(1-x)e^{-\frac{m_b+m_c}{8m_b m_c\omega}\left(\frac{m_c^2}{x} + \frac{m_b^2}{1-x}\right)}, \tag{10}$$

with the shape parameter $\omega = 0.5 \pm 0.1$ GeV related to the factor N_B by the normalization

$$\int_0^1 \phi_{B_c}(x)dx = 1. \tag{11}$$

For the P-wave charmonium states, we use the abbreviations A, S, and T correspond to axial-vector, scalar, and tensor charmonium meson, respectively. In terms of the notation in Ref. [54], the nonlocal matrix element for the longitudinally and transversely polarized axial-vector and scalar charmonium meson can be decomposed as

$$\begin{aligned}
&\langle A(P_2,\epsilon_{2L})|\bar{c}_\alpha(z)c_\beta(0)|0\rangle \\
&=\frac{1}{\sqrt{2N_c}}\int_0^1 dx e^{ixP_2\cdot z}[m_2\gamma_5\not{\epsilon}_{2L}\psi_A^L(x)+\gamma_5\not{\epsilon}_{2L}\not{P}_2\psi_A^t(x)]_{\beta\alpha}, \\
&\langle A(P_2,\epsilon_{2T})|\bar{c}_\alpha(z)c_\beta(0)|0\rangle \\
&=\frac{1}{\sqrt{2N_c}}\int_0^1 dx e^{ixP_2\cdot z}[m_2\gamma_5\not{\epsilon}_{2T}\psi_A^V(x)+\gamma_5\not{\epsilon}_{2T}\not{P}_2\psi_A^T(x)]_{\beta\alpha}, \\
&\langle S(P_2)|\bar{c}_\alpha(z)c_\beta(0)|0\rangle \\
&=\frac{1}{\sqrt{2N_c}}\int_0^1 dx e^{ixP_2\cdot z}[\not{P}_2\psi_S^v(x)+m_2\psi_S^s(x)]_{\beta\alpha},
\end{aligned} \tag{12}$$

where the DAs $\psi^{L,T,v}(x)$ are of twist-2, and $\psi^{t,V,s}(x)$ of twist-3. As mentioned in the Introduction, the charmonium DAs are parametrized using a combination of an universal factor $\mathcal{T}(x)$ for the P-wave states and the asymptotic models $\Phi_{\rm asy}(x)$, given by

$$\psi^i \propto \Phi^i_{\rm asy}(x)\mathcal{T}(x). \tag{13}$$

The expression of $\mathcal{T}(x)$ can be extracted from P-wave Schrödinger states for a Coulomb potential, which are derived in the Appendix. The asymptotic forms of $\Phi^i_{\rm asy}(x)$ in Eq. (13) for the axial-vector mesons can be related to the ones calculated in QCD sum rules by [55]

$$\begin{aligned}
&\Phi_A^L(x)=\frac{f_A}{2\sqrt{2N_c}}\phi_\parallel(x), \qquad &&\Phi_A^T(x)=\frac{f_A^\perp}{2\sqrt{2N_c}}\phi_\perp(x), \\
&\Phi_A^t(x)=\frac{f_A^\perp}{2\sqrt{2N_c}}h_\parallel^{(t)}(x), \qquad &&\Phi_A^V(x)=\frac{f_A}{2\sqrt{2N_c}}g_\perp^{(a)}(x),
\end{aligned} \tag{14}$$

where f_A ($f_A^\perp$) is the vector (tensor) decay constants. The leading twist $\phi_{\parallel,\perp}$ can be expanded in a series of Gegenbauer polynomials [55,56]

$$\begin{aligned}
\phi_\parallel &= 6x(1-x)[a_0^\parallel+3a_1^\parallel(2x-1)+\cdots], \\
\phi_\perp &= 6x(1-x)[a_0^\perp+3a_1^\perp(2x-1)+\cdots].
\end{aligned} \tag{15}$$

Owing to the G-parity, $\phi_\parallel$ ($\phi_\perp$) for $^3P_1$ state is symmetric (antisymmetric) under the exchange of quark and antiquark momentum fractions in the SU(3) limit. On the contrary, $\phi_\parallel$ is antisymmetric for $^1P_1$ states, while $\phi_\perp$ is symmetric in this case. Thus the asymptotic forms for twist-2 can be written as

$$\begin{aligned}
&\phi_\parallel(x)=6a_0^\parallel x(1-x), \\
&\phi_\perp(x)=18a_1^\perp x(1-x)(2x-1) \quad \text{for } ^3P_1; \\
&\phi_\parallel(x)=18a_1^\parallel x(1-x)(2x-1), \\
&\phi_\perp(x)=6a_0^\perp x(1-x) \quad \text{for } ^1P_1.
\end{aligned} \tag{16}$$

Neglecting the three-parton distribution amplitudes containing gluons and terms proportional to light quark masses, the twist-3 DAs can be related to the twist-2 ones by Wandzura-Wilczek-type relations [55]:

$$\begin{aligned}
g_\perp^{(a)}(x) &= \frac{1}{2}\left[\int_0^x du\frac{\phi_\parallel(u)}{1-u}+\int_x^1 dv\frac{\phi_\parallel(u)}{u}\right], \\
h_\parallel^{(t)}(x) &= (2x-1)\left[\int_0^x du\frac{\phi_\perp(u)}{1-u}-\int_x^1 dv\frac{\phi_\perp(u)}{u}\right],
\end{aligned} \tag{17}$$

which further give

$$\begin{aligned}
&h_\parallel^{(t)}(x)=3a_1^\perp(2x-1)(1-6x+6x^2), \\
&g_\perp^{(a)}(x)=\frac{3}{4}a_0^\parallel(1+(2x-1)^2) \quad \text{for } ^3P_1; \\
&h_\parallel^{(t)}(x)=3a_0^\perp(2x-1)^2, \\
&g_\perp^{(a)}(x)=\frac{3}{2}a_1^\parallel(2x-1)^3 \quad \text{for } ^1P_1.
\end{aligned} \tag{18}$$

Combining Eqs. (14), (16), and (18), we derive

$$\begin{aligned}
\psi^L(x) &= \frac{f_A}{2\sqrt{2N_c}}N_L x(1-x)\mathcal{T}(x), \\
\psi^T(x) &= \frac{f_A^\perp}{2\sqrt{2N_c}}N_T x(1-x)(2x-1)\mathcal{T}(x), \\
\psi^t(x) &= \frac{f_A^\perp}{2\sqrt{2N_c}}\frac{N_T}{6}(2x-1)[1-6x+6x^2]\mathcal{T}(x), \\
\psi^V(x) &= \frac{f_A}{2\sqrt{2N_c}}\frac{N_L}{8}[1+(1-2x)^2]\mathcal{T}(x),
\end{aligned} \tag{19}$$

for $^3P_1$ states, and

$$\begin{aligned}
\psi^L(x) &= \frac{f_A}{2\sqrt{2N_c}}N_T x(1-x)(2x-1)\mathcal{T}(x), \\
\psi^T(x) &= \frac{f_A^\perp}{2\sqrt{2N_c}}N_L x(1-x)\mathcal{T}(x), \\
\psi^t(x) &= \frac{f_A^\perp}{2\sqrt{2N_c}}\frac{N_L}{2}(1-2x)^2\mathcal{T}(x), \\
\psi^V(x) &= \frac{f_A}{2\sqrt{2N_c}}\frac{N_T}{12}(2x-1)^3\mathcal{T}(x),
\end{aligned} \tag{20}$$

for $^1P_1$ states. Note that the Gegenbauer moments $a_{0,1}^{\parallel,\perp}$ are absorbed into the coefficients $N_{L,T}$ to satisfy the normalization conditions [57]

$$\begin{aligned}
&\int_0^1 N_L x(1-x)\mathcal{T}(x)dx=1, \\
&\int_0^1 N_T x(1-x)(2x-1)^2\mathcal{T}(x)dx=1.
\end{aligned} \tag{21}$$

Because of the charge conjugation invariance, twist-2 and twist-3 DAs of the scalar meson should satisfy $\psi_S^v(x)=-\psi_S^v(1-x)$ and $\psi_S^s(x)=\psi_S^s(1-x)$, respectively [58,59]. In general, the asymptotic twist-2 DA can also be expanded

in the Gegenbauer polynomials with only odd component contribute [60,61]. Based on the description of the charmonium states DAs given above, $\psi_S^v(x)$ can be recast to the form

$$\psi_S^v(x) = \frac{f_S}{2\sqrt{2N_c}} N_T x(1-x)(2x-1)\mathcal{T}(x). \quad (22)$$

As for the twist-3 DA, we adopt the same asymptotic form as the pseudoscalar mesons [62]:

$$\psi_S^s(x) = \frac{f_S}{2\sqrt{2N_c}} N_S \mathcal{T}(x), \quad (23)$$

with the normalization condition

$$\int_0^1 \psi_S^s(x)dx = \frac{f_S}{2\sqrt{2N_c}}. \quad (24)$$

The nonlocal matrix element associating with the tensor charmonium can be decomposed as [63]

$$\begin{aligned}
&\langle T(P_2,\epsilon_{\bullet L})|\bar{c}_\alpha(z)c_\beta(0)|0\rangle \\
&\quad = \frac{1}{\sqrt{2N_c}}\int_0^1 dx e^{ixP_2\cdot z}[m_2 \not{\epsilon}_{\bullet L}\psi_T(x) + \not{\epsilon}_{\bullet L}\not{P}_2\psi_T^t(x)]_{\beta\alpha}, \\
&\langle T(P_2,\epsilon_{\bullet T})|\bar{c}_\alpha(z)c_\beta(0)|0\rangle \\
&\quad = \frac{1}{\sqrt{2N_c}}\int_0^1 dx e^{ixP_2\cdot z}[m_2 \not{\epsilon}_{\bullet T}\psi_T^V(x) + \not{\epsilon}_{\bullet T}\not{P}_2\psi_T^T(x)]_{\beta\alpha},
\end{aligned} \quad (25)$$

for the longitudinal and transverse polarizations, respectively. $\psi_T(x)$, $\psi_T^T(x)$ are leading twist DAs, and $\psi_T^V(x)$, $\psi_T^t(x)$ are twist-3 ones, which are related to the ones given in Ref. [46]

$$\begin{aligned}
\Phi_T(x) &= \frac{f_T}{2\sqrt{2N_c}}\phi_\parallel(x), \\
\Phi_T^T(x) &= \frac{f_T^\perp}{2\sqrt{2N_c}}\phi_\perp(x), \\
\Phi_T^t(x) &= \frac{f_T^\perp}{2\sqrt{2N_c}}h_\parallel^{(t)}(x), \\
\Phi_T^V(x) &= \frac{f_T}{2\sqrt{2N_c}}g_\perp^{(v)}(x).
\end{aligned} \quad (26)$$

In SU(3) limit, due to the G-parity of the tensor meson, all of the DAs are antisymmetric under the replacement $x \to 1-x$. Here we take the following approximate forms of twist-2 as [46,63]

$$\phi_\parallel(x) = \phi_\perp(x) = N_T x(1-x)(2x-1), \quad (27)$$

and the corresponding expressions for the twist-3 DAs can be derived through the Wandzura-Wilczek relations as [46]

$$\begin{aligned}
h_\parallel^{(t)}(x) &= \frac{N_T}{4}(2x-1)(1-6x+6x^2), \\
g_\perp^{(v)}(x) &= \frac{N_T}{6}(2x-1)^3.
\end{aligned} \quad (28)$$

Now we can collect the DAs of tensor charmonium states below:

$$\begin{aligned}
\psi_T(x) &= \frac{f_T}{2\sqrt{2N_c}}N_T x(1-x)(2x-1)\mathcal{T}(x), \\
\psi_T^T(x) &= \frac{f_T^\perp}{2\sqrt{2N_c}}N_T x(1-x)(2x-1)\mathcal{T}(x), \\
\psi_T^t(x) &= \frac{f_T^\perp}{2\sqrt{2N_c}}\frac{N_T}{4}(2x-1)[1-6x+6x^2]\mathcal{T}(x), \\
\psi_T^V(x) &= \frac{f_T}{2\sqrt{2N_c}}\frac{N_T}{6}(2x-1)^3\mathcal{T}(x),
\end{aligned} \quad (29)$$

with the normalization conditions [46]

$$\int_0^1 (2x-1)\psi_T^{(T)}(x) = \frac{f_T^{(\perp)}}{2\sqrt{2N_c}}. \quad (30)$$

For the wave functions of light pseudoscalar and vector mesons, the same forms and parameters are adopted as [52] and one is referred to the original literature [64].

C. The decay amplitudes

In the PQCD approach, the decay amplitudes are expressed as the convolution of the hard kernels H with the relevant meson wave functions Φ_i

$$\begin{aligned}
&\mathcal{A}(B_c \to M_2M_3) \\
&\quad = \int d^4k_1 d^4k_2 d^4k_3 \mathrm{Tr}[C(t)\Phi_1(k_1)\Phi_2(k_2) \\
&\qquad \times \Phi_3(k_3)H(k_1,k_2,k_3,t)].
\end{aligned} \quad (31)$$

"Tr" denotes the trace over all Dirac structures and color indices. The hadron wave functions Φ_i absorbed all the nonperturbative components have been described in Sec. II B. The hard kernel $H(k_1,k_2,k_3,t)$ describes the four quark operator and the spectator quark connected by a hard gluon, which can be perturbatively calculated including all possible Feynman diagrams without end-point singularity. In the following, we start to compute the decay amplitudes of the concerned decays.

1. Amplitudes for $B_c \to (S,A,T)P$ decays

We mark subscript S, A, and T to denote the decay amplitudes contain a scalar, axial-vector, and tensor charmonium in the final states, respectively. The amplitudes from factorizable diagrams (a) and (b) in Fig. 1 for $B_c \to SP, AP$ decays read as

$$\begin{aligned}\mathcal{F}_S &= 2\sqrt{\frac{2}{3}}C_F f_B f_P \pi M^4 (r_2^2-1)\int_0^1\int_0^1 dx_1 dx_2 \int_0^\infty\int_0^\infty b_1 b_2 db_1 db_2 \phi_{B_c}(x_1)\\ &\times [r_2\psi_S^s(x_2,b_2)(r_b-2x_2)+\psi_S^v(x_2,b_2)(x_2-2r_b)]E_{ab}(t_a)h(\alpha_e,\beta_a,b_1,b_2)S_t(x_2)-\\ &\times [\psi_S^v(x_2,b_2)(r_c+r_2^2(x_1-1))-2r_2\psi_S^s(x_2,b_2)(r_c+x_1-1)]E_{ab}(t_b)h(\alpha_e,\beta_b,b_2,b_1)S_t(x_1),\end{aligned} \tag{32}$$

$$\begin{aligned}\mathcal{F}_A &= -2\sqrt{\frac{2}{3}}C_F f_B f_P \pi M^4 (r_2^2-1)\int_0^1\int_0^1 dx_1 dx_2 \int_0^\infty\int_0^\infty b_1 b_2 db_1 db_2 \phi_{B_c}(x_1)\\ &\times [r_2\psi_A^t(x_2,b_2)(r_b-2x_2)+\psi_A^L(x_2,b_2)(x_2-2r_b)]E_{ab}(t_a)h(\alpha_e,\beta_a,b_1,b_2)S_t(x_2)\\ &+\psi_A^L(x_2,b_2)[r_c+r_2^2(x_1-1)]E_{ab}(t_b)h(\alpha_e,\beta_b,b_2,b_1)S_t(x_1),\end{aligned} \tag{33}$$

respectively. The corresponding formula for nonfactorizable diagrams (c) and (d) are

$$\begin{aligned}\mathcal{M}_S &= \frac{8}{3}C_F f_B \pi M^4 (r_2^2-1)\int_0^1\int_0^1\int_0^1 dx_1 dx_2 dx_3 \int_0^\infty\int_0^\infty b_1 b_3 db_1 db_3 \phi_{B_c}(x_1)\phi_P^A(x_3)\\ &\times [\psi_S^v(x_2,b_1)(r_2^2(x_1+2x_2+x_3-2)+x_1-x_3)-r_2\psi_S^s(x_2,b_1)(x_1+x_2-1)]E_{cd}(t_c)h(\beta_c,\alpha_e,b_3,b_1)\\ &-[\psi_S^v(x_2,b_1)(r_2^2(x_2-x_3)+2x_1+x_2+x_3-2)-r_2\psi_S^s(x_2,b_1)(x_1+x_2-1)]E_{cd}(t_d)h(\beta_d,\alpha_e,b_3,b_1),\end{aligned} \tag{34}$$

$$\begin{aligned}\mathcal{M}_A &= \frac{8}{3}C_F f_B \pi M^4 (r_2^2-1)\int_0^1\int_0^1\int_0^1 dx_1 dx_2 dx_3 \int_0^\infty\int_0^\infty b_1 b_3 db_1 db_3 \phi_{B_c}(x_1)\phi_P^A(x_3)\\ &\times [\psi_A^L(x_2,b_1)(r_2^2-1)(x_1-x_3)-r_2\psi_A^t(x_2,b_1)(x_1+x_2-1)]E_{cd}(t_c)h(\beta_c,\alpha_e,b_3,b_1)\\ &+[\psi_A^L(x_2,b_1)(r_2^2(x_2-x_3)+2x_1+x_2+x_3-2)-r_2\psi_A^t(x_2,b_1)(x_1+x_2-1)]E_{cd}(t_d)h(\beta_d,\alpha_e,b_3,b_1),\end{aligned} \tag{35}$$

with $r_{b,c}=m_{b,c}/M$. $C_F=4/3$ is a color factor. f_P is the decay constant of the light pseudoscalar meson, emitted from the weak vertex. The functions h, E and the factorization scales $t_{a,b,c,d}$ can be found in [42]. The leading twist DAs of the pseudoscalar meson ϕ_P^A and the jet function $S_t(x)$ come from [52]. α_e and $\beta_{a,b,c,d}$ are the virtuality of the internal gluon and quarks, respectively. Their expressions are

$$\begin{aligned}\alpha_e &= -[x_1-(1-x_2)r_2^2](x_1+x_2-1)M^2,\\ \beta_a &= [r_b^2-x_2(1+r_2^2(x_2-1))]M^2,\\ \beta_b &= [r_c^2+(x_1-1)(r_2^2-x_1)]M^2,\\ \beta_c &= -(x_1+x_2-1)[x_1-x_3+r_2^2(x_2+x_3-1)]M^2,\\ \beta_d &= -(x_1+x_2-1)[x_1+x_3-1+r_2^2(x_2-x_3)]M^2.\end{aligned} \tag{36}$$

It should be stressed that the nonlocal matrix element for the axial-vector and scalar charmonium meson in Eq. (12) can be related to the vector and pseudoscalar ones [42,43], respectively, by multiplying by the structure $-(i)\gamma_5$ from the left hand. The factorization formulas ($\mathcal{F}/\mathcal{M}$) here and below are similar to the corresponding ones in [42,43] with some terms flipping signs. As mentioned before, the nonlocal matrix element associating with the tensor charmonium in Eq. (25) is also analogous to the vector case, except that the polarization vector is replaced by $\epsilon_{\bullet}$. Therefore the correspondence between a tensor meson and a axial-vector meson allows us to get the factorization formulas of $B_c \to TP$ as

$$\begin{aligned}\mathcal{F}_T &= \sqrt{\frac{2}{3}}\mathcal{F}_A|_{\psi_A^L\to\psi_T,\psi_A^t\to\psi_T^t,r_c\to -r_c},\\ \mathcal{M}_T &= \sqrt{\frac{2}{3}}\mathcal{M}_A|_{\psi_A^L\to\psi_T,\psi_A^t\to\psi_T^t}.\end{aligned} \tag{37}$$

With the functions obtained in the above, the total decay amplitudes for the $B_c \to (S,A,T)P$ are given by

$$\begin{aligned}&\mathcal{A}(B_c\to(S,A,T)P)\\ &= V_{cb}^* V_{uq}\left[\left(C_2+\frac{1}{3}C_1\right)\mathcal{F}_{S,A,T}+C_1\mathcal{M}_{S,A,T}\right].\end{aligned} \tag{38}$$

2. Amplitudes for $B_c \to (S,A,T)V$ decays

For $B_c \to SV$ decays, the decay amplitudes of factorization emission diagrams and nonfactorization emission diagrams are given as

$$\mathcal{F}_S = 2\sqrt{\frac{2}{3}}C_F f_B f_V \pi M^4 \sqrt{1-r_2^2}\int_0^1\int_0^1 dx_1dx_2\int_0^\infty\int_0^\infty b_1b_2db_1db_2\phi_{B_c}(x_1)$$
$$\times [r_2\psi_S^s(x_2,b_2)(r_b-2x_2)+\psi_S^v(x_2,b_2)(x_2-2r_b)]E_{ab}(t_a)h(\alpha_e,\beta_a,b_1,b_2)S_t(x_2)$$
$$-[\psi_S^v(x_2,b_2)(r_c+r_2^2(x_1-1))-2r_2\psi_S^s(x_2,b_2)(r_c+x_1-1)]E_{ab}(t_b)h(\alpha_e,\beta_b,b_2,b_1)S_t(x_1), \quad (39)$$

$$\mathcal{M}_S = \frac{8}{3}C_F f_B \pi M^4\sqrt{1-r_2^2}\int_0^1\int_0^1\int_0^1 dx_1dx_2dx_3\int_0^\infty\int_0^\infty b_1b_3db_1db_3\phi_{B_c}(x_1)\phi_V(x_3)$$
$$\times[\psi_S^v(x_2,b_1)(r_2^2(x_1+2x_2+x_3-2)+x_1-x_3)-r_2\psi_S^s(x_2,b_1)(x_1+x_2-1)]E_{cd}(t_c)h(\beta_c,\alpha_e,b_3,b_1)$$
$$-[\psi_S^v(x_2,b_1)(r_2^2(x_2-x_3)+2x_1+x_2+x_3-2)-r_2\psi_S^s(x_2,b_1)(x_1+x_2-1)]E_{cd}(t_d)h(\beta_d,\alpha_e,b_3,b_1), \quad (40)$$

where f_V and ϕ_V are the decay constants and the twist-2 distribution amplitudes of the light vector mesons, respectively. The total decay amplitudes for $B_c \to SV$ decays are similar to that of $B_c \to SP$ in Eq. (38) with the replacement $f_P \to f_V$, $\phi_P^A \to \phi_V$.

Like vector mesons, axial-vector mesons also carry spin degrees of freedom. Therefore, $B_c \to AV$ decays contain more amplitudes associated with three different polarizations. We mark superscript L, N and T to denote the contributions from longitudinal polarization, normal polarization, and transverse polarization, respectively.

$$\mathcal{F}_A^L = 2\sqrt{\frac{2}{3}}C_F f_B f_V \pi M^4\sqrt{1-r_2^2}\int_0^1\int_0^1 dx_1dx_2\int_0^\infty\int_0^\infty b_1b_2db_1db_2\phi_{B_c}(x_1)$$
$$\times[r_2\psi_A^t(x_2,b_2)(r_b-2x_2)+\psi_A^L(x_2,b_2)(x_2-2r_b)]E_{ab}(t_a)h(\alpha_e,\beta_a,b_1,b_2)S_t(x_2)$$
$$+\psi_A^L(x_2,b_2)[r_c+r_2^2(x_1-1)]E_{ab}(t_b)h(\alpha_e,\beta_b,b_2,b_1)S_t(x_1), \quad (41)$$

$$\mathcal{F}_A^N = 2\sqrt{\frac{2}{3}}C_F f_B f_V r_3 \pi M^4\int_0^1\int_0^1 dx_1dx_2\int_0^\infty\int_0^\infty b_1b_2db_1db_2\phi_{B_c}(x_1)$$
$$\times[\psi_A^T(x_2,b_2)(r_2^2(r_b+2-4x_2)+r_b-2)+r_2\psi_A^V(x_2,b_2)(r_2^2(x_2-1)+x_2+1)-4r_b]$$
$$\times E_{ab}(t_a)h(\alpha_e,\beta_a,b_1,b_2)S_t(x_2)-\psi_A^V(x_2,b_2)r_2[1-2r_c-2x_1+r_2^2]E_{ab}(t_b)h(\alpha_e,\beta_b,b_2,b_1)S_t(x_1), \quad (42)$$

$$\mathcal{F}_A^T = 2\sqrt{\frac{2}{3}}C_F f_B f_V r_3 \pi M^4(r_2^2-1)\int_0^1\int_0^1 dx_1dx_2\int_0^\infty\int_0^\infty b_1b_2db_1db_2\phi_{B_c}(x_1)$$
$$\times[\psi_A^T(x_2,b_2)(2-r_b)+r_2\psi_A^V(x_2,b_2)(x_2-1)]$$
$$\times E_{ab}(t_a)h(\alpha_e,\beta_a,b_1,b_2)S_t(x_2)+\psi_A^V(x_2,b_2)r_2E_{ab}(t_b)h(\alpha_e,\beta_b,b_2,b_1)S_t(x_1), \quad (43)$$

$$\mathcal{M}_A^L = \frac{8}{3}C_F f_B \pi M^4\sqrt{1-r_2^2}\int_0^1\int_0^1\int_0^1 dx_1dx_2dx_3\int_0^\infty\int_0^\infty b_1b_3db_1db_3\phi_{B_c}(x_1)\phi_V(x_3)$$
$$\times[-\psi_A^L(x_2,b_1)(r_2^2-1)(x_1-x_3)+r_2\psi_A^t(x_2,b_1)(x_1+x_2-1)]E_{cd}(t_c)h(\beta_c,\alpha_e,b_3,b_1)-$$
$$\times[\psi_A^L(x_2,b_1)(r_2^2(x_2-x_3)+2x_1+x_2+x_3-2)-r_2\psi_A^t(x_2,b_1)(x_1+x_2-1)]E_{cd}(t_d)h(\beta_d,\alpha_e,b_3,b_1), \quad (44)$$

$$\mathcal{M}_A^N = \frac{8}{3}C_F f_B r_3 \pi M^4\int_0^1\int_0^1\int_0^1 dx_1dx_2dx_3\int_0^\infty\int_0^\infty b_1b_3db_1db_3\phi_{B_c}(x_1)$$
$$\times[\phi_V^a(x_3)\psi_A^V(x_2,b_1)(r_2^2-1)(x_2+x_3-1)+\phi_V^v(x_3)\psi_A^T(x_2,b_1)(r_2^2(x_1+2x_2+x_3-2)+x_1-x_3)]$$
$$\times E_{cd}(t_c)h(\beta_c,\alpha_e,b_3,b_1)+[\phi_V^a(x_3)2(r_2^2-1)(r_2(x_2-x_3)\psi_A^V(x_2,b_1)+2(x_1+x_3-1)\psi_A^T(x_2,b_1))$$
$$+\phi_V^v(x_3)(2r_2\psi_A^V(x_2,b_1)(r_2^2(x_2-x_3)+2x_1+x_2+x_3-2)$$
$$+\psi_A^T(x_2,b_1)(r_2^2(1-x_1-2x_2+x_3)+1-x_1-x_3))]E_{cd}(t_d)h(\beta_d,\alpha_e,b_3,b_1), \quad (45)$$

$$\mathcal{M}_A^T = -\frac{8}{3} C_F f_B r_3 \pi M^4 \int_0^1\int_0^1\int_0^1 dx_1 dx_2 dx_3 \int_0^\infty\int_0^\infty b_1 b_3 db_1 db_3 \phi_{B_c}(x_1)$$
$$\times [\phi_V^a(x_3)\psi_A^V(x_2,b_1)2r_2(r_2^2(x_2+x_3-1)+2x_1+x_2-x_3-1)+\phi_V^v(x_3)\psi_A^T(x_2,b_1)(r_2^2-1)(x_1-x_3)]$$
$$\times E_{cd}(t_c)h(\beta_c,\alpha_e,b_3,b_1)+[2\phi_V^a(x_3)(r_2\psi_A^V(x_2,b_1)(r_2^2(x_2-x_3)+2x_1+x_2+x_3-2)$$
$$+2\psi_A^T(x_2,b_1)(r_2^2(1-x_1-2x_2+x_3)+1-x_1-x_3))$$
$$+\phi_V^v(x_3)\psi_A^T(x_2,b_1)(r_2^2-1)(x_1+x_3-1)]E_{cd}(t_d)h(\beta_d,\alpha_e,b_3,b_1), \quad (46)$$

where ϕ_V^a and ϕ_V^v are the two twist-3 distribution amplitudes for the transverse polarization of light vector mesons. For $B_c \to TV$ decays, the decay amplitudes can be related to the axial-vector ones by making the following replacement,

$$\mathcal{F}(\mathcal{M})_T^L = \sqrt{\frac{2}{3}}\mathcal{F}(\mathcal{M})_A^L|_{\psi_A^L\to\psi_T,\psi_A^t\to\psi_T^t,r_c\to -r_c},$$
$$\mathcal{F}(\mathcal{M})_T^{N,T} = \sqrt{\frac{1}{2}}\mathcal{F}(\mathcal{M})_A^{N,T}|_{\psi_A^T\to\psi_T^T,\psi_A^V\to\psi_T^V,r_c\to -r_c}, \quad (47)$$

where the factors $\sqrt{\frac{2}{3}}$ and $\sqrt{\frac{1}{2}}$ come from the equivalent polarization vector $\epsilon_\bullet$ in Eq. (8) of the tensor mesons for the longitudinal and transverse polarizations, respectively. The total decay amplitudes for $B_c \to (A,T)V$ decays can be decomposed as

$$\mathcal{A}(B_c \to (A,T)V) = \mathcal{A}_{A,T}^L + \mathcal{A}_{A,T}^N \epsilon_{2T}\cdot\epsilon_{3T} + i\mathcal{A}_{A,T}^T \epsilon_{\alpha\beta\rho\sigma} n^\alpha v^\beta \epsilon_{2T}^\rho \epsilon_{3T}^\sigma, \quad (48)$$

where the three polarization amplitudes have the same structure as Eq. (38).

III. NUMERICAL RESULTS

To proceed the numerical analysis, it is useful to summarize all of the input quantities we have used in this work. The central values (in GeV) of the relevant meson masses and heavy quark masses are adopted as [1]

$$M = 6.275, \quad m_b = 4.8, \quad m_c = 1.275,$$
$$m_\rho = 0.775, \quad m_{K^*} = 0.892. \quad (49)$$

While the masses of the P-wave charmonium have been given in Table I. The CKM matrix-elements are set as $|V_{cb}| = 0.0405$, $|V_{us}| = 0.2248$, and $|V_{ud}| = 0.97417$ [1]. For the decay constants of P-wave charmonium, the detailed discussions in the nonrelativistic QCD factorization, the light-front approach and the QCD sum rules, could be found in Refs. [57,65–67]. Here we employ the most recent updated values (in GeV) evaluated from the QCD sum rules at the scale $\mu = m_c$ [67]:

$$f_{\chi_{c0}} = 0.0916, \quad f_{\chi_{c1}} = 0.185,$$
$$f_{\chi_{c2}} = 0.177, \quad f_{h_c} = 0.127,$$
$$f_{\chi_{c1}}^\perp = 0.0875, \quad f_{\chi_{c2}}^\perp = 0.128, \quad f_{h_c}^\perp = 0.133. \quad (50)$$

For the decay constants of light mesons, we use [52]

$$f_\pi = 0.131, \quad f_K = 0.160, \quad f_\rho = 0.209,$$
$$f_{K^*} = 0.217, \quad f_\rho^\perp = 0.165, \quad f_{K^*}^\perp = 0.185 \text{ GeV}. \quad (51)$$

The B_c meson decay constant and lifetime are adopted as $f_{B_c} = 0.489$ GeV [42,43] and $\tau_{B_c} = 0.507$ ps [1], respectively.

The branching ratios for the considered decays in the B_c meson rest frame can be written as

$$\mathcal{B} = \frac{G_F^2 \tau_{B_c}}{32\pi M}(1-r_2^2)|\mathcal{A}|^2, \quad (52)$$

where the decay amplitudes $\mathcal{A}$ for each channel have been given explicitly in the previous section. When the final states involve axial-vector/tensor charmonium states and a vector meson, the decay amplitude can be decomposed into three components,

$$|\mathcal{A}|^2 = |\mathcal{A}_0|^2 + |\mathcal{A}_\parallel|^2 + |\mathcal{A}_\perp|^2, \quad (53)$$

where $\mathcal{A}_0$, $\mathcal{A}_\parallel$, $\mathcal{A}_\perp$ refer to the longitudinal, parallel, and perpendicular polarization amplitudes in the transversity basis, respectively, which are related to $\mathcal{A}^{L,N,T}$ of Eq. (48) via

$$\mathcal{A}_0 = \mathcal{A}^L, \quad \mathcal{A}_\parallel = \sqrt{2}\mathcal{A}^N, \quad \mathcal{A}_\perp = \sqrt{2}\mathcal{A}^T. \quad (54)$$

Our numerical results of branching ratios for $B_c \to (S,A,T)P$ and $B_c \to (S,A,T)V$ decays are listed in Tables II and III, respectively. The first kind of uncertainties is from the shape parameter ω in the wave function of the B_c meson and the charm-quark mass m_c. In the evaluation, we vary the value of ω within a 20% range and $m_c = 1.275$ GeV by ± 0.025 GeV. The second error comes from the decay constants of the P-wave charmonium meson in Eq. (50), which varies 10% for error estimates. The last one is caused by the hard scale t located between $0.75 \sim 1.25$ times the invariant masses of the internal particles, which

TABLE II. The PQCD predictions on branching ratios of B_c decays to final states containing a P-wave charmonium state and a light pseudoscalar meson. The errors for these entries correspond to the uncertainties in hadronic shape parameters, from the decay constants, and the scale dependence, respectively. For comparison, we also list other theoretical results. Note that some branching ratios are evaluated with the Wilson coefficient $a_1 = 1.14$ in the referred models.

Modes	This work	[30]	[31]	[33]	[35]	[36]	[37]	[41]
$B_c^+ \to \chi_{c0}\pi^+$	$(1.6^{+0.2+0.3+0.0}_{-0.2-0.3-0.1}) \times 10^{-3}$	2.1×10^{-4}	2.6×10^{-4}	5.5×10^{-4}	2.8×10^{-4}	9.8×10^{-3}	3.1×10^{-4}	4.2×10^{-3}
$B_c^+ \to \chi_{c1}\pi^+$	$(5.1^{+0.3+1.1+0.0}_{-0.4-1.1-0.2}) \times 10^{-4}$	2.0×10^{-4}	1.4×10^{-6}	6.8×10^{-5}	7.0×10^{-5}	8.9×10^{-5}	2.1×10^{-5}	5.0×10^{-5}
$B_c^+ \to \chi_{c2}\pi^+$	$(4.0^{+0.3+0.9+0.3}_{-0.4-0.8-0.3}) \times 10^{-3}$	3.8×10^{-4}	2.2×10^{-4}	4.6×10^{-4}	2.5×10^{-4}	7.9×10^{-3}	2.1×10^{-4}	7.4×10^{-4}
$B_c^+ \to h_c\pi^+$	$(5.4^{+0.4+1.0+0.4}_{-0.3-1.0-0.3}) \times 10^{-4}$	4.6×10^{-4}	5.3×10^{-4}	1.1×10^{-3}	5.0×10^{-4}	1.6×10^{-2}	9.8×10^{-4}	6.2×10^{-3}
$B_c^+ \to \chi_{c0}K^+$	$(1.2^{+0.2+0.3+0.0}_{-0.2-0.2-0.1}) \times 10^{-4}$	1.6×10^{-5}	2.0×10^{-5}	4.2×10^{-5}	2.1×10^{-6}	…	2.3×10^{-5}	3.2×10^{-4}
$B_c^+ \to \chi_{c1}K^+$	$(3.8^{+0.3+0.9+0.1}_{-0.3-0.8-0.1}) \times 10^{-5}$	1.5×10^{-5}	1.1×10^{-7}	5.1×10^{-6}	5.2×10^{-7}	…	1.6×10^{-6}	4.0×10^{-6}
$B_c^+ \to \chi_{c2}K^+$	$(3.1^{+0.3+0.7+0.2}_{-0.2-0.6-0.2}) \times 10^{-4}$	2.8×10^{-5}	1.7×10^{-5}	3.4×10^{-5}	1.8×10^{-6}	…	1.6×10^{-5}	5.6×10^{-5}
$B_c^+ \to h_cK^+$	$(4.3^{+0.3+0.7+0.3}_{-0.2-0.8-0.2}) \times 10^{-5}$	3.5×10^{-5}	4.1×10^{-5}	8.3×10^{-5}	3.8×10^{-6}	…	7.4×10^{-5}	4.7×10^{-4}

characterizes the size of higher-order corrections to the hard amplitudes. It turns out that the errors are dominant by the uncertainties from the decay constants of P-wave charmonium meson distribution amplitudes, which can reach 20% in magnitude. As discussed in Ref. [68], by using the light-cone wave function for the B_c meson, the theoretical uncertainty from the charm-quark mass is largely reduced. It is also found that the branching ratios are insensitive to the hard scale, which means the higher-order contributions can be safely neglected. In a recent paper [69], the authors claimed that the relativistic corrections to light-cone distribution amplitudes of S-wave heavy quarkonia are comparable with the next-to-leading order radiative corrections. In view of this point, we check the sensitivity of our results to the squared velocity v^2 of the charm quark inside the P-wave charmonium states in Eq. (A6). The variation of v^2 in the range $0.25 \sim 0.35$ will result in the branching ratios changing only a few percents. This is similar to the comment in [34] that the relativistic corrections to the Coulomb wave functions would be less significant. In addition, the uncertainties related to the light mesons, such as the decay constants and the Gegenbauer moments shown in [52], are less than 10%. Therefore, they have been neglected in our calculations.

It can be seen that the former four processes (including one π or ρ meson in the final states) have relatively large branching ratios owing to the CKM factor enhancement, while the branching ratios of the latter four processes (including one K or K^* meson in the final states) are comparatively small due to the CKM factor suppression. Since the two type decays have identical topology and similar kinematic properties. In the limit of SU(3) flavor symmetry, the relative ratios $\mathcal{R}_{K/\pi} \equiv \mathcal{B}(B_c \to (S,A,T)K)/\mathcal{B}(B_c \to (S,A,T)\pi)$ and $\mathcal{R}_{K^*/\rho} \equiv \mathcal{B}(B_c \to (S,A,T)K^*)/\mathcal{B}(B_c \to (S,A,T)\rho)$ are dominated by the ratio of the relevant CKM matrix elements $|V_{us}|^2/|V_{ud}|^2 \sim \lambda^2$ under the naive factorization approximation. After including the kaon (K^*) and pion (ρ) decay constants, one expects

TABLE III. The PQCD predictions on branching ratios of B_c decays to final states containing a P-wave charmonium state and a light vector meson. The errors for these entries correspond to the uncertainties in hadronic shape parameters, from the decay constants, and the scale dependence, respectively. For comparison, we also list other theoretical results. Note that some branching ratios are evaluated with the Wilson coefficient $a_1 = 1.14$ in the referred models.

Modes	This work	[30]	[31]	[33]	[35]	[36]	[37]	[38]
$B_c^+ \to \chi_{c0}\rho^+$	$(5.8^{+0.6+1.1+0.4}_{-0.6-1.2-0.4}) \times 10^{-3}$	5.8×10^{-4}	6.7×10^{-4}	1.3×10^{-3}	7.2×10^{-4}	3.3×10^{-2}	7.6×10^{-4}	…
$B_c^+ \to \chi_{c1}\rho^+$	$(2.8^{+0.2+0.5+0.1}_{-0.2-0.5-0.1}) \times 10^{-3}$	1.5×10^{-4}	1.0×10^{-4}	2.9×10^{-4}	2.9×10^{-4}	4.6×10^{-3}	2.3×10^{-4}	1.47×10^{-3}
$B_c^+ \to \chi_{c2}\rho^+$	$(1.6^{+0.1+0.4+0.1}_{-0.1-0.3-0.0}) \times 10^{-2}$	1.1×10^{-3}	6.5×10^{-4}	1.2×10^{-3}	5.1×10^{-4}	3.2×10^{-2}	5.6×10^{-4}	…
$B_c^+ \to h_c\rho^+$	$(2.3^{+0.1+0.3+0.2}_{-0.2-0.4-0.1}) \times 10^{-3}$	1.0×10^{-3}	1.3×10^{-3}	2.5×10^{-3}	1.2×10^{-3}	5.3×10^{-2}	2.2×10^{-3}	1.24×10^{-3}
$B_c^+ \to \chi_{c0}K^{*+}$	$(3.3^{+0.4+0.7+0.2}_{-0.3-0.6-0.2}) \times 10^{-4}$	4.0×10^{-5}	3.7×10^{-5}	7.0×10^{-5}	3.9×10^{-6}	…	4.5×10^{-5}	…
$B_c^+ \to \chi_{c1}K^{*+}$	$(1.8^{+0.2+0.3+0.3}_{-0.1-0.3-0.1}) \times 10^{-4}$	1.0×10^{-5}	7.3×10^{-6}	1.8×10^{-5}	1.8×10^{-6}	…	1.7×10^{-5}	7.07×10^{-5}
$B_c^+ \to \chi_{c2}K^{*+}$	$(9.6^{+0.7+2.0+0.6}_{-0.8-1.8-0.4}) \times 10^{-4}$	7.4×10^{-5}	3.8×10^{-5}	6.5×10^{-5}	3.1×10^{-6}	…	3.3×10^{-5}	…
$B_c^+ \to h_cK^{*+}$	$(1.3^{+0.1+0.3+0.2}_{-0.1-0.2-0.0}) \times 10^{-4}$	7.0×10^{-5}	7.1×10^{-5}	1.3×10^{-4}	6.8×10^{-6}	…	1.3×10^{-4}	6.18×10^{-5}

$\mathcal{R}_{K/\pi} \sim 0.081$ and $\mathcal{R}_{K^*/\rho} \sim 0.057$. From Tables II and III, our predictions for $\mathcal{R}_{K/\pi}$ corresponding to various P-wave charmonium states lie in the range 0.075 to 0.080, while $\mathcal{R}_{K^*/\rho}$ is in the range 0.057 to 0.064, both are very close to the above expected values. It means that the dominant contributions to the branching ratios come from the factorizable topology, while the nonfactorizable contribution is suppressed by the Wilson coefficient C_1 [see Eq. (38)].

One can see some interesting hierarchical relations among these branching ratios in our predictions. For example, branching ratios for decays involving pseudoscalar mesons in the final state are smaller than their vector partners for the same flavor content. This is partially due to the pseudoscalar meson decay constant is usual smaller than the vector ones. Furthermore, since the B_c meson is a spinless particle, according to the angular momentum conservation, only one partial wave contribute to the $B_c \to SP, AP, TP, SV$ decays, while in the AV, TV modes, three partial waves are simultaneously allowed, resulting in the larger branching ratios. For those channels with the same light meson and different P-wave charmonium mesons in the final states, we have the following hierarchy pattern:

$$\mathcal{B}(B_c \to \chi_{c2}P) > \mathcal{B}(B_c \to \chi_{c0}P) > \mathcal{B}(B_c \to \chi_{c1}P) \sim \mathcal{B}(B_c \to h_cP). \quad (55)$$

As discussed in Ref. [43], the branching ratio of $B_c \to \eta_c(2S)\pi$ is enhanced by the twist-3 distribution amplitude from Fig. 3(b). Nevertheless, this contribution vanishes for $B_c \to \psi(2S)\pi$ decay since the Lorentz structure of the vector charmonium wave functions is different from the pseudoscalar case. As mentioned in the previous section, because of the corresponding relation between a pseudoscalar (vector) and a scalar (axial-vector) charmonium, the similar situation also exists in this work. The twist-3 distribution amplitude from Fig 1(b) also give the dominant contribution to the $B_c \to \chi_{c0}P$ decays, while for other channels, the dominant contribution still come from the twist-2 ones. Because the strong interference between the twist-2 and twist-3 contributions is constructive in $B_c \to \chi_{c0}P$, we have a large branching ratio for this mode. One can see that the dominant twist-2 contributions for $B_c \to (\chi_{c1}, h_c)P$ are suppressed by a factor of $r_c - r_2^2$ given in Eq. (33), whereas this suppression is absent in the case of $B_c \to \chi_{c2}P$ due to the r_c term flipping sign [see Eq. (37)]. This explains why $B_c \to \chi_{c2}P$ has a rate greater than $\chi_{c1}P$ and h_cP. Of course, this is only a rough estimate on the magnitudes, the branching ratios also have been related to the decay constants and the distribution amplitudes of the various P-wave charmonium mesons. The relations between the decay constants $f_{\chi_{c2}} > f_{\chi_{c0}}$ in Eq. (50) implies that $\mathcal{B}(B_c \to \chi_{c2}P) > \mathcal{B}(B_c \to \chi_{c0}P)$. The similar pattern also occurs $B_c \to (A, S, T)V$ decays; see Table III.

As mentioned in the Introduction, many other work have performed a systematic study on the P-wave charmonium decays of B_c mesons. Various approaches such as several relativistic and nonrelativistic quark models [30,31,33,35], the sum rules of QCD [36], the improved Bethe-Salpeter approach [37], the Isgur-Scora-Grinstein-Wise II model [38], and the nonrelativistic QCD effective theory [41] have been used to calculate the branching ratios. For the sake of comparison, we briefly list the obtained theoretical results in Tables II and III. One finds that some of the results given by different models are roughly comparable. For example, our theoretical predictions on those decays involving the h_c meson in the final state are of the same order of magnitude as observed in [30,31,33,37]. The branching ratios of $B_c \to \chi_{c1}\pi$ and $B_c \to h_c\pi$ evaluated by N. Sharma *et al.* [70] are 7×10^{-4} and 6×10^{-4}, respectively, which also match well with our results. In a very recent paper [71], the author predicted the branching ratio $\mathcal{B}(B_c^+ \to \chi_{c0}\pi^+) = 1.22 \times 10^{-3}$, which is comparable to our prediction. Of course, some predicted values are quite a spread in various models. The predictions in Ref. [36] are typically larger excepted for $B_c^+ \to \chi_{c1}\pi^+$. Previously, Castro *et al.* [72] studied the nonleptonic decays of the B_c into tensor mesons using the factorization hypothesis. They predict $\mathcal{B}(B_c \to \chi_{c2}\pi)$, $\mathcal{B}(B_c \to \chi_{c2}K)$, $\mathcal{B}(B_c \to \chi_{c2}\rho)$, and $\mathcal{B}(B_c \to \chi_{c2}K^*)$, as 7.5×10^{-5}, 5.49×10^{-6}, 2.38×10^{-4}, and 1.33×10^{-5}, respectively, which are considerably smaller than our results as well as most of other model calculations. Our results for a final $K^{(*)}$ are also larger than those of other approaches. The disagreement in the predictions may be attributed to the different values of the form factors used in these approaches. Experimental investigations on these decays may be used to test theoretical methods according to their predictions.

On the experimental side, so far only the evidence for the decay $B_c^+ \to \chi_{c0}\pi^+$ is found at 4.0σ significance by the LHCb Collaboration [17]. The ratio of production cross sections of the B_c^+ and B^+ mesons times branching fractions is measured to be $\frac{\sigma_{B_c^+}}{\sigma_{B^+}} \times \mathcal{B}(B_c^+ \to \chi_{c0}\pi^+) = (9.8^{+3.4}_{-3.0}(\text{stat}) \pm 0.8(\text{syst})) \times 10^{-6}$ [17]. As a cross-check, the cross section ratio $\frac{\sigma_{B_c^+}}{\sigma_{B^+}}$ can be extracted from another charmonium mode, $\frac{\sigma_{B_c^+}}{\sigma_{B^+}} \times \frac{\mathcal{B}(B_c^+ \to J/\psi\pi^+)}{\mathcal{B}(B^+ \to J/\psi K^+)} = (0.683 \pm 0.018 \pm 0.009)\%$ measured by the LHCb Collaboration [73]. The branching ratio $\mathcal{B}(B^+ \to J/\psi K^+)$, determined from the world average value, is $(1.026 \pm 0.031) \times 10^{-3}$ [1]. If we use our previous PQCD calculation $\mathcal{B}(B_c^+ \to J/\psi\pi^+) = (2.33^{+0.81}_{-0.61}) \times 10^{-3}$ [42], where all errors are combined in quadrature, as an input, the ratio $\frac{\sigma_{B_c^+}}{\sigma_{B^+}}$ is in the region of $(2.2 \sim 4.1) \times 10^{-3}$. Combined with the prediction on $\mathcal{B}(B_c^+ \to \chi_{c0}\pi^+)$ in Table II, we obtain the range $\frac{\sigma_{B_c^+}}{\sigma_{B^+}} \times \mathcal{B}(B_c^+ \to \chi_{c0}\pi^+) = (2.6 \sim 8.2) \times 10^{-6}$, which is consistent with the LHCb data with one sigma errors.

TABLE IV. The PQCD predictions for the polarization fractions, relative phases in the $B_c \to (A,T)V$ decays. The errors induced by the same sources as in Table II.

Modes	f_0	$f_\parallel$	$f_\perp$	$\phi_\parallel$(rad)	$\phi_\perp$(rad)
$B_c^+ \to \chi_{c1}\rho^+$	$0.66^{+0.03+0.04+0.00}_{-0.02-0.04-0.00}$	$0.15^{+0.02+0.03+0.00}_{-0.01-0.02-0.00}$	$0.18^{+0.03+0.03+0.01}_{-0.01-0.02-0.00}$	$1.21^{+0.06+0.08+0.01}_{-0.04-0.09-0.01}$	$1.67^{+0.04+0.04+0.00}_{-0.04-0.04-0.01}$
$B_c^+ \to \chi_{c1}K^{*+}$	$0.60^{+0.03+0.05+0.02}_{-0.03-0.04-0.00}$	$0.18^{+0.02+0.02+0.00}_{-0.02-0.03-0.01}$	$0.22^{+0.02+0.03+0.00}_{-0.01-0.03-0.00}$	$1.22^{+0.06+0.08+0.00}_{-0.04-0.10-0.03}$	$1.68^{+0.04+0.04+0.01}_{-0.05-0.04-0.01}$
$B_c^+ \to \chi_{c2}\rho^+$	$0.93^{+0.01+0.01+0.00}_{-0.02-0.02-0.01}$	$0.05^{+0.00+0.01+0.00}_{-0.00-0.01-0.00}$	$0.03^{+0.00+0.00+0.00}_{-0.01-0.01-0.01}$	$1.00^{+0.06+0.01+0.01}_{-0.04-0.02-0.02}$	$1.12^{+0.05+0.01+0.02}_{-0.05-0.01-0.04}$
$B_c^+ \to \chi_{c2}K^{*+}$	$0.90^{+0.01+0.01+0.01}_{-0.00-0.01-0.01}$	$0.06^{+0.01+0.01+0.01}_{-0.00-0.00-0.00}$	$0.03^{+0.00+0.01+0.01}_{-0.00-0.00-0.00}$	$1.00^{+0.06+0.03+0.01}_{-0.03-0.01-0.02}$	$1.12^{+0.06+0.01+0.02}_{-0.05-0.00-0.04}$
$B_c^+ \to h_c\rho^+$	$0.91^{+0.01+0.02+0.01}_{-0.01-0.02-0.01}$	$0.04^{+0.01+0.01+0.00}_{-0.01-0.02-0.01}$	$0.05^{+0.01+0.01+0.01}_{-0.01-0.00-0.00}$	$0.83^{+0.05+0.02+0.00}_{-0.05-0.03-0.01}$	$1.11^{+0.04+0.02+0.01}_{-0.04-0.03-0.01}$
$B_c^+ \to h_cK^{*+}$	$0.88^{+0.01+0.02+0.01}_{-0.01-0.00-0.00}$	$0.05^{+0.01+0.00+0.00}_{-0.01-0.01-0.01}$	$0.07^{+0.01+0.00+0.00}_{-0.01-0.01-0.01}$	$0.85^{+0.05+0.01+0.00}_{-0.05-0.01-0.01}$	$1.13^{+0.04+0.02+0.01}_{-0.04-0.02-0.01}$

Turning to the polarizations for $B_c \to AV, TV$ decays. We usually define five observables corresponding to three polarization fractions $f_\lambda(\lambda = 0, \parallel, \perp)$, and two relative phases $\phi_\parallel$, $\phi_\perp$, where

$$f_\lambda = \frac{|\mathcal{A}_\lambda|^2}{|\mathcal{A}_0|^2 + |\mathcal{A}_\parallel|^2 + |\mathcal{A}_\perp|^2}, \qquad \phi_{\parallel,\perp} = \arg\frac{\mathcal{A}_{\parallel,\perp}}{\mathcal{A}_0}, \quad (56)$$

with normalization such that $\sum_\lambda f_\lambda = 1$. The results for the polarization fractions and their relative phases are displayed in Table IV, where the sources of the errors in the numerical estimates have the same origin as in the discussion of the branching ratios in Table II. It can be observed that both the polarization fractions and the phases are relatively stable with respect to the variations of hadronic parameters, the decay constants and the hard scale, and therefore they serve as good quantities to test the standard model. Several remarks are given in order. First, the contributions to the branching ratios mainly arise from the longitudinal polarizations because of the relation $f_0 \gg f_\parallel \sim f_\perp$, which is expected from the power counting rules. For example, the longitudinal parts of $B_c \to TV$ decays occupy over 90%, which are very similar to the case of $B_c \to J/\psi V$ [42]. However, the longitudinal polarizations of $B_c \to \chi_{c1}V$ are relative smaller (∼60%) compared to that of $B_c \to h_cV$. As mentioned before, owing to the G-parity, the distribution amplitudes for χ_{c1} and h_c mesons exhibit the different asymptotic behaviors (see Eqs. (19) and (20)). If we use the h_c distribution amplitudes for calculation, the resultant predictions $f_0(\chi_{c1}V)$ can be increase to around 90%. Besides, the longitudinal and transverse decay constants in the two axial-vector mesons can also contribute to different polarizations. Second, for $B_c \to (A,T)\rho$ and $B_c \to (A,T)K^*$ decays, both have similar magnitudes and phases of the amplitudes, which suggests the SU(3) breaking effect between them is small. Last, the predicted relative phases deviations from π indicate the existence of the still unknown final-state interaction. However, the magnitudes and phases of the two transverse amplitudes $\mathcal{A}_\parallel$ and $\mathcal{A}_\perp$ are roughly equal, which is expected from analyses based on quark-helicity conservation [74,75]. These results and findings will be further tested by the LHCb and Belle-II experiments in the near future.

IV. CONCLUSION

The two-body B_c meson decays to a P-wave charmonium state $(\chi_{c0}, \chi_{c1}, \chi_{c2}, h_c)$ and a light (π, K, ρ, K^*) meson are systematically analysed within the perturbative QCD approach. Our predictions for the branching ratios are summarized in Tables II and III and compared with other theoretical results. Overall, the predicted branching ratios from different theoretical models have a relative big spread. The upcoming experimental measurements of the corresponding decay rates can examine various theoretical approaches. Based on our estimations, the dominating decay mode of the concerned processes is $B_c \to \chi_{c2}\rho$ with predicted branching ratios of 1.6%, which should be accessible experimentally at high-luminosity hadron colliders. We also estimate the polarization contributions in $B_c \to (\chi_{c1,c2}, h_c)V$ decays. As expected, based on the factorization assumption, the longitudinal polarization dominates and the transverse polarizations are of the same size.

We also discussed theoretical uncertainties arising from the hadronic parameters in B_c meson wave function, the decay constants of charmonium states and the hard scale t. The branching ratios suffer a large error from the decay constants, whereas the polarization observables are less sensitive to these parameters. The obtained results can be confronted to the experimental data in the future.

ACKNOWLEDGMENTS

I would like to acknowledge Hsiang-nan Li and Yu-Ming Wang for helpful discussions. This work is supported in part by the National Natural Science Foundation of China under Grants No. 11547020 and No. 11605060 and, in part, by the Program for the Top Young Innovative Talents of Higher Learning Institutions of Hebei Educational Committee under Grant No. BJ2016041.

APPENDIX: DETAILS FOR DERIVING THE *P*-WAVE CHARMONIUM DAS

Starting with the momentum-space radial wave function which can be written as the Fourier transform of the position-space expression $\psi_{nlm}(\vec{r})$

$$\psi(k) = \int_{-\infty}^{\infty} \psi_{nlm}(\vec{r}) e^{-i\vec{k}\cdot\vec{r}} d\vec{r}, \tag{A1}$$

where n, l, and m stand for main, orbital, and magnetic quantum numbers, respectively. In above equation, the first term $\psi_{nlm}(\vec{r})$ is known to be separated into $R_{nl}(r)Y_{lm}(\theta,\varphi)$ in the spherical coordinates (r, θ, φ), while the second exponential term in the plane wave expansion can be written as

$$e^{-i\vec{k}\cdot\vec{r}} = e^{-ikr\cos\theta} = \sum_{l'=0}^{\infty} \sqrt{4\pi(2l'+1)}(-i)^{l'} j_{l'}(kr) Y_{l'0}(\theta,0), \tag{A2}$$

with $j_{l'}(kr)$ the spherical Bessel function. We then write Eq. (A1) as

$$\psi(k) = \sqrt{4\pi(2l+1)}(-i)^{l} \int_0^{\infty} j_l(kr) R_{nl}(r) r^2 dr, \tag{A3}$$

where the orthogonality property $\int_0^{\pi}\int_0^{2\pi} Y_{lm} Y_{l'0} \sin\theta d\theta d\varphi = \delta_{ll'}\delta_{m0}$ have been used.

For the *P*-wave states $n = 2$ and $l = 1$, employing the spherical Bessel function $j_1(kr) = \frac{\sin(kr) - kr\cos(kr)}{(kr)^2}$ and the radial wave function for a Coulomb Potential $R_{21}(r) \propto re^{\frac{-q_B r}{2}}$, the integral of Eq. (A3) evaluates to

$$\psi(k) \propto \frac{kq_B}{(4k^2 + q_B^2)^3}, \tag{A4}$$

where q_B is the Bohr momentum. Note that the above expression is in contrast to Eq. (47) in [54]. We argue that the spherical harmonics function for *P*-wave states is dependent on the angle θ, which should contribute to the integral in Eq. (A1). In particular, Eq. (A4) is almost the same as M. Beneke's calculation in Ref. [76] (see Eq. (45)), except for a constant term which can be absorbed in the redefinition of the wave function of the *P*-wave charmonium. Following much the same procedure as described in Refs. [44,54], we obtain the heavy quarkonium DA which is dependent on the charm quark momentum fraction x after integrating the transverse momentum k_T,

$$\Phi(x) \sim \int d^2k_T \psi(x,k_T) \propto x(1-x) \times \left\{ \frac{\sqrt{x(1-x)(1-4x(1-x))^3}}{[1-4x(1-x)(1-v^2/4)]^2} \right\}, \tag{A5}$$

where $v = q_B/m_c$ is the charm quark velocity. In the numerical calculation, we take $v^2 = 0.3$ and neglect the v^2 term in the numerator [54]. As mentioned in Eq. (13), we propose the *P*-wave charmonium states DAs as $\psi(x) \propto \Phi_{\rm asy}(x)\mathcal{T}(x)$ with

$$\mathcal{T}(x) = \left\{ \frac{\sqrt{x(1-x)(1-4x(1-x))^3}}{[1-4x(1-x)(1-v^2/4)]^2} \right\}^{1-v^2}, \tag{A6}$$

where the power $1 - v^2$ denotes the small relativistic corrections to the Coulomb wave functions [44].

[1] C. Patrignani *et al.* (Particle Data Group), Chin. Phys. C **40**, 100001 (2016).
[2] R. Kumar *et al.* (Belle Collaboration), Phys. Rev. D **74**, 051103(R) (2006).
[3] R. Kumar *et al.* (Belle Collaboration), Phys. Rev. D **78**, 091104 (2008).
[4] K. Abe *et al.* (Belle Collaboration), Phys. Rev. Lett. **88**, 031802 (2002).
[5] B. Aubert *et al.* (*BABAR* Collaboration), Phys. Rev. D **78**, 091101(R) (2008).
[6] K. Abe *et al.* (Belle Collaboration), Phys. Rev. Lett. **89**, 011803 (2002).
[7] B. Aubert *et al.* (*BABAR* Collaboration), Phys. Rev. Lett. **94**, 141801 (2005).
[8] B. Aubert *et al.* (*BABAR* Collaboration), Phys. Rev. Lett. **102**, 132001 (2009).
[9] N. Soni *et al.* (Belle Collaboration), Phys. Lett. B **634**, 155 (2006).
[10] V. Bhardwaj *et al.* (Belle Collaboration), Phys. Rev. Lett. **107**, 091803 (2011).
[11] F. Fang *et al.* (Belle Collaboration), Phys. Rev. D **74**, 012007 (2006).
[12] B. Aubert *et al.* (*BABAR* Collaboration), Phys. Rev. D **78**, 012006 (2008).
[13] R. Aaij *et al.* (LHCb Collaboration), Nucl. Phys. **B874**, 663 (2013).
[14] J. P. Lees *et al.* (*BABAR* Collaboration), Phys. Rev. D **85**, 052003 (2012).
[15] V. Bhardwaj *et al.* (Belle Collaboration), Phys. Rev. D **93**, 052016 (2016).
[16] R. Aaij *et al.* (LHCb Collaboration), Phys. Rev. Lett. **119**, 062001 (2017).

[17] R. Aaij *et al.* (LHCb Collaboration), Phys. Rev. D **94**, 091102(R) (2016).
[18] C. H. Chang and Y. Q. Chen, Phys. Rev. D **49**, 3399 (1994).
[19] J. F. Liu and K. T. Chao, Phys. Rev. D **56**, 4133 (1997).
[20] A. Abd El-Hady, J. H. Munoz, and J. P. Vary, Phys. Rev. D **62**, 014019 (2000).
[21] P. Colangelo and F. De Fazio, Phys. Rev. D **61**, 034012 (2000).
[22] V. V. Kiselev, A. E. Kovalsky, and A. K. Likhoded, Nucl. Phys. **B585**, 353 (2000).
[23] D. Ebert, R. N. Faustov, and V. O. Galkin, Phys. Rev. D **68**, 094020 (2003).
[24] H. Fu, Y. Jiang, C. S. Kim, and G. L. Wang, J. High Energy Phys. 06 (2011) 015.
[25] Sk. Naimuddin, S. Kar, M. Priyadarsini, N. Barik, and P. C. Dash, Phys. Rev. D **86**, 094028 (2012).
[26] S. Kar, P. C. Dash, M. Priyadarsini, Sk. Naimuddin, and N. Barik, Phys. Rev. D **88**, 094014 (2013).
[27] C.-F. Qiao, P. Sun, D. Yang, and R.-L. Zhu, Phys. Rev. D **89**, 034008 (2014).
[28] H. W. Ke, T. Liu, and X. Q. Li, Phys. Rev. D **89**, 017501 (2014).
[29] C. H. Chang, H. F. Fu, G. L. Wang, and J. M. Zhang, Sci. China Phys. Mech. Astron. **58**, 1 (2015).
[30] D. Ebert, R. N. Faustov, and V. O. Galkin, Phys. Rev. D **82**, 034019 (2010).
[31] E. Hernández, J. Nieves, and J. M. Verde-Velasco, Phys. Rev. D **74**, 074008 (2006).
[32] M. A. Ivanov, J. G. Körner, and P. Santorelli, Phys. Rev. D **71**, 094006 (2005).
[33] M. A. Ivanov, J. G. Körner, and P. Santorelli, Phys. Rev. D **73**, 054024 (2006).
[34] Y. M. Wang and C. D. Lü, Phys. Rev. D **77**, 054003 (2008).
[35] C. H. Chang, Y. Q. Chen, G. L. Wang, and H. S. Zong, Phys. Rev. D **65**, 014017 (2001); Commun. Theor. Phys. **35**, 395 (2001).
[36] V. V. Kiselev, O. N. Pakhomova, and V. A. Saleev, J. Phys. G **28**, 595 (2002).
[37] Z.-h. Wang, G.-L. Wang, and C.-H. Chang, J. Phys. G **39**, 015009 (2012).
[38] R. Dhir and C. S. Kim, Phys. Rev. D **87**, 034004 (2013).
[39] X.-X. Wang, W. Wang, and C. D. Lü, Phys. Rev. D **79**, 114018 (2009).
[40] Q. Li, T.-h. Wang, Y. Jiang, H. Yuan, and G.-L. Wang, Eur. Phys. J. C **76**, 454 (2016).
[41] R. Zhu, arXiv:1710.07011.
[42] Z. Rui and Z. T. Zou, Phys. Rev. D **90**, 114030 (2014).
[43] Z. Rui, W. F. Wang, G. X. Wang, L. H. Song, and C. D. Lü, Eur. Phys. J. C **75**, 293 (2015).
[44] A. E. Bondar and V. L. Chernyak, Phys. Lett. B **612**, 215 (2005).
[45] G. Buchalla, A. J. Buras, and M. E. Lautenbacher, Rev. Mod. Phys. **68**, 1125 (1996).
[46] H. Y. Cheng, Y. Koike, and K. C. Yang, Phys. Rev. D **82**, 054019 (2010).
[47] H. Y. Cheng and K.-C. Yang, Phys. Rev. D **83**, 034001 (2011).
[48] M. Beneke, G. Buchalla, M. Neubert, and C. T. Sachrajda, Nucl. Phys. **B591**, 313 (2000).
[49] A. G. Grozin and M. Neubert, Phys. Rev. D **55**, 272 (1997).
[50] M. Beneke and T. Feldmann, Nucl. Phys. **B592**, 3 (2001).
[51] C. D. Lü and M. Z. Yang, Eur. Phys. J. C **28**, 515 (2003).
[52] A. Ali, G. Kramer, Y. Li, C. D. Lü, Y. L. Shen, W.Wang, and Y. M. Wang, Phys. Rev. D **76**, 074018 (2007).
[53] J. Sun, Y. Yang, Q. Chang, and G. Lu, Phys. Rev. D **89**, 114019 (2014).
[54] C.-H. Chen and H.-N. Li, Phys. Rev. D **71**, 114008 (2005).
[55] K.-C. Yang, Nucl. Phys. **B776**, 187 (2007).
[56] K. C. Yang, J. High Energy Phys. 10 (2005) 108.
[57] X. P. Wang and D. Yang, J. High Energy Phys. 06 (2014) 121.
[58] V. L. Chernyak and A. R. Zhitnitsky, Phys. Rep. **112**, 173 (1984).
[59] M. Diehl and G. Hiller, J. High Energy Phys. 06 (2001) 067.
[60] C.-H. Chen, Phys. Rev. D **67**, 094011 (2003).
[61] W. Wang, Y.-L. Shen, Y. Li, and C.-D. Lü, Phys. Rev. D **74**, 114010 (2006).
[62] H. Y. Cheng, C.-K. Chua, and K. C. Yang, Phys. Rev. D **73**, 014017 (2006).
[63] W. Wang, Phys. Rev. D **83**, 014008 (2011).
[64] V. M. Braun and I. E. Filyanov, Z. Phys. C **48**, 239 (1990); P. Ball, V. M. Braun, Y. Koike, and K. Tanaka, Nucl. Phys. **B529**, 323 (1998); P. Ball, J. High Energy Phys. 01 (1999) 010.
[65] C. W. Hwang, J. High Energy Phys. 10 (2009) 074.
[66] V. V. Braguta, A. K. Likhoded, and A. V. Luchinsky, Phys. Rev. D **79**, 074004 (2009).
[67] M. A. Olpak, A. Ozpineci, and V. Tanriverdi, Phys. Rev. D **96**, 014026 (2017).
[68] Z. Rui, H. Li, G. X. Wang, and Y. Xiao, Eur. Phys. J. C **76**, 564 (2016).
[69] W. Wang, J. Xu, D. Yang, and S. Zhao, J. High Energy Phys. 12 (2017) 012.
[70] N. Sharma, R. Dhir, and R C Verma, J. Phys. G **37**, 075013 (2010).
[71] B. Mohammadi, J. High Energy Phys. 12 (2017) 019.
[72] G. L. Castro, H. B. Mayorga, and J. H. Muñoz, J. Phys. G **28**, 2241 (2002).
[73] R. Aaij *et al.* (LHCb Collaboration), Phys. Rev. Lett. **114**, 132001 (2015).
[74] A. Ali, J. G. Körner, G. Kramer, and J. Willrodt, Z. Phys. C **1**, 269 (1979).
[75] M. Suzuki, Phys. Rev. D **64**, 117503 (2001).
[76] M. Beneke and L. Vernazza, Nucl. Phys. **B811**, 155 (2009).